

Article

Temporal Evolution of Urban Heat Island and Quantitative Relationship with Urbanization Development in Chongqing, China

Junmiao Zhang , Liu Tian and Jun Lu * 

School of Civil Engineering, Chongqing University, Chongqing 400044, China

* Correspondence: lujun@cqu.edu.cn

Abstract: Urban development always has a strong impact on the urban thermal environment, but it is unclear to what extent urbanization factors influence urban heat island intensity (UHII) in mountainous cities, and fewer studies have been conducted on the trends of long-term UHII in mountainous cities. Chongqing, as the only municipality directly under the central government in Southwest China and a typical mountainous city, is chosen as the case study. This study analyzed the interannual and seasonal variations of UHII based on the data from meteorological stations in Chongqing from 1959 to 2018 using the least-squares method and the Mann–Kendall test, and explored the relationship between urbanization factors (urban resident population, gross domestic product (GDP), fixed investments, and gross industrial output value) and UHII. The results show that the increasing rates of temperature in urban areas of Chongqing are significantly higher than those in rural areas affected by urbanization. Using the Mann–Kendall test, it is found that almost all abrupt temperature changes in Chongqing occurred after the rapid urbanization of Chongqing in the 21st century. The annual mean UHII increased from 0.1 °C to 1.5 °C during the study period, with summer making the largest contribution. It is also found that the UHII in Chongqing has increased year by year, especially after the 1980s. The increasing rates of UHII are larger at night and smaller during the day. The increasing trends of nighttime UHII are statistically significant, while those of daytime UHII are not. In addition, UHII and urbanization factors are found to be correlated using the grey relational analysis (GRA). Eventually, a comprehensive UHII index and a comprehensive urbanization index are constructed using principal component analysis (PCA). A tertiary regression model of UHII and urbanization index is established, which reflects that the UHII in Chongqing will continue to grow rapidly with the development of the city.

Keywords: mountainous city; temporal characteristics; urban climate; urbanization development; urban heat island



Citation: Zhang, J.; Tian, L.; Lu, J. Temporal Evolution of Urban Heat Island and Quantitative Relationship with Urbanization Development in Chongqing, China. *Atmosphere* **2022**, *13*, 1594. <https://doi.org/10.3390/atmos13101594>

Academic Editors: Riccardo Buccolieri, Jian Hang, Liyue Zeng and Cho Kwong Charlie Lam

Received: 28 July 2022

Accepted: 22 September 2022

Published: 29 September 2022

Publisher's Note: MDPI stays neutral with regard to jurisdictional claims in published maps and institutional affiliations.



Copyright: © 2022 by the authors. Licensee MDPI, Basel, Switzerland. This article is an open access article distributed under the terms and conditions of the Creative Commons Attribution (CC BY) license (<https://creativecommons.org/licenses/by/4.0/>).

1. Introduction

Urbanization is an essential stage of a country's development. In 2018, 55% of the world's population lived in cities, and that number is expected to reach 68% by 2050 according to World Urbanization Prospects [1]. Urbanization has significantly transformed natural and semi-natural surfaces into impermeable urban structures, disrupting the balance of radiation and energy on the Earth's surface and the composition of near-surface atmospheric structures [2]. The sensible and latent heat fluxes in urbanized areas will also change, leading to the urban heat island phenomenon (UHI) [3]. Therefore, the formation of UHI is the ecological result of urbanization [4]. Urban heat island intensity (UHII) inevitably increases with the acceleration of urbanization, and the areas affected by UHI are gradually expanding [5]. It is well known that the formation of UHI has a series of adverse impacts on the urban ecosystem, such as a rise in energy consumption demand for cooling in summers, air pollution, and global warming, reduced comfort of citizens and

increased levels of human morbidity and mortality. Therefore, investigating UHI and the relationship between UHI and urbanization is important.

Currently, meteorological data analysis, observational approaches (including fixed or mobile monitoring), remote sensing, and numerical simulation are the most widely used approaches to understand the characteristics of UHI [6–8]. Meteorological data analysis can use long-term data to study the variability of UHI. Nevertheless, it is impossible to comprehensively and accurately reflect the urban thermal environment due to the spatial scarcity and uneven distribution of meteorological stations [9]. Observation approaches can directly obtain continuous spatial meteorological data, but the results can be influenced by factors such as vehicles and pedestrians [10]. The remote sensing approach has the advantages of a large observation range and good visualization. However, it is limited by low temporal resolution and interference from clouds [11,12]. Moreover, the remote sensing data represent the surface temperature rather than the air temperature. Numerical simulation can study the coupling relations between UHI and variables. However, given the complexity of the study area, several simplifications of the model need to be applied that might compromise the accuracy and reliability of the results [13].

Many studies have been conducted to understand the characteristics of UHI using the above methods. Li et al. [14] used the data of four meteorological stations in Lanzhou in the past 60 years to study the multiscale characteristics of UHI. Liu et al. [15] used the data (2009–2018) of 37 automatic meteorological stations in Beijing to study the effect of urbanization on UHI. Sumita et al. [16] quantified the impact of LULC changes on UHI intensity in northwest India using WRF. Helen et al. [17] analyzed winter UHI in the West Midlands (UK) using WRF and estimated the impact on cold-related mortality. Yao et al. [18] explored the trend of summer UHI footprint in the Beijing metropolitan region and its relationship with urbanization factors based on the Landsat series and MODIS datasets. Muhammad et al. [19] used the satellite thermal band of the Landsat dataset to calculate LST and evaluated the influence of wind on SUHI. Samuel et al. [20] analyzed the UHI intensity in different urban areas of Zaragoza (Spain) and the temporal variability of UHI using hourly observatories composed of 21 sensors. Francois et al. [21] recorded the air temperature in 13 LCZs of Nancy (France) by mobile measurements and analyzed the influence of urban structure on urban climate for UHI assessment.

China has experienced rapid urbanization and dramatic economic development with huge impacts on the climate in recent decades [22]. From 1978 to 2018, the urban population increased from 172.5×10^6 to 813.5×10^6 . The urbanization rate increased from 17.9% to 58.5% in China [23]. Recent studies in China reported that the UHI has linearly increased over the past 30 years. Owing to great urbanization and significant UHI, cities in China provide unique information on the interplay between urbanization and UHI. Nevertheless, present studies on UHI are mainly focused on lowland cities, but few studies are conducted on mountainous cities. Chongqing is a typical mountainous city in western China. The following are some representative studies conducted in Chongqing: Liu and Li [24] studied the spatial and temporal characteristics of summer UHI intensity and its relationship with land cover in Chongqing from 2007 to 2016 based on Landsat 5 TM and Landsat 8 TIRS. Jiang et al. [25] analyzed the daily and seasonal variation characteristics of UHI in Chongqing using the data from 55 automatic meteorological stations in 2017. Liao et al. [26] investigated the spatial distribution of UHI in Chongqing using MODIS LST data and meteorological observation data. Using Landsat 8 OLI images, Liu et al. [27] found that the sky view factor and industrial areas contributed significantly to UHI in Chongqing, while Wang et al. [28] found vegetation cover and urban surface elevation played a greater role. Zhu et al. [29] used MODIS LST data to compare the distribution characteristics of UHI in areas with and without sponge city planning.

Previous studies on UHI in Chongqing have mainly focused on the spatial distribution and short-term temporal variability of UHI, while long-term and comprehensive research on UHI has barely been addressed. In addition, most studies on the factors influencing the urban heat island effect have also focused on the relationship between UHI and land

cover or used the nighttime light index to represent the urbanization level and to study its correlation with UHI [25]. Less effort has been put into the quantitative relations between urbanization factors and UHI in Chongqing.

To address these issues, in this paper, the least-squares method and the Mann–Kendall test are used to analyze the seasonal and annual temperature (mean/maximum/minimum) and UHI (mean/maximum/minimum) characteristics in Chongqing through the data of urban and rural meteorological stations from 1959 to 2018, and the grey relational analysis and principal component analysis method are used to explore the quantitative relationship between urbanization factors and UHI intensity. The results can provide a scientific basis for urban ecological environment construction in Chongqing.

2. Materials and Methods

2.1. Materials

2.1.1. Study Area

Chongqing, known as the mountain city, is the only municipality directly under the central and western parts of China. Chongqing covers 82,401 km², of which 732 km² could be classified as Central Districts of Chongqing in 2018. Located in the southwest part of China and the southeast edge of the Sichuan Basin, it spans the transition zone between the Qinghai–Tibet Plateau and the Middle-Lower Yangtze plain. The longitude and latitude ranges are 28°10′–32°13′ N and 105°11′–110°11′ E, respectively. The terrain slopes from the south to the Yangtze River valley. The landform is dominated by hills and mountains; mountains account for 76%. It has a humid subtropical monsoon climate with an annual average temperature of 16–18 °C.

2.1.2. Data

The long-term meteorological data were collected from the National Meteorological Information Center (<http://data.cma.cn/>) (accessed on 2 September 2020), including data from the Shapingba meteorological station in the central urban areas and the Hechuan meteorological station in rural areas of Chongqing from 1959 to 2018 (Figure 1). The selection principle of meteorological representative stations in central urban and rural areas is mainly determined according to the accumulation time and continuity of meteorological data and location and relocation of meteorological stations [30]. These stations were selected from National Principal Meteorological Stations, and their details are illustrated in Table 1.

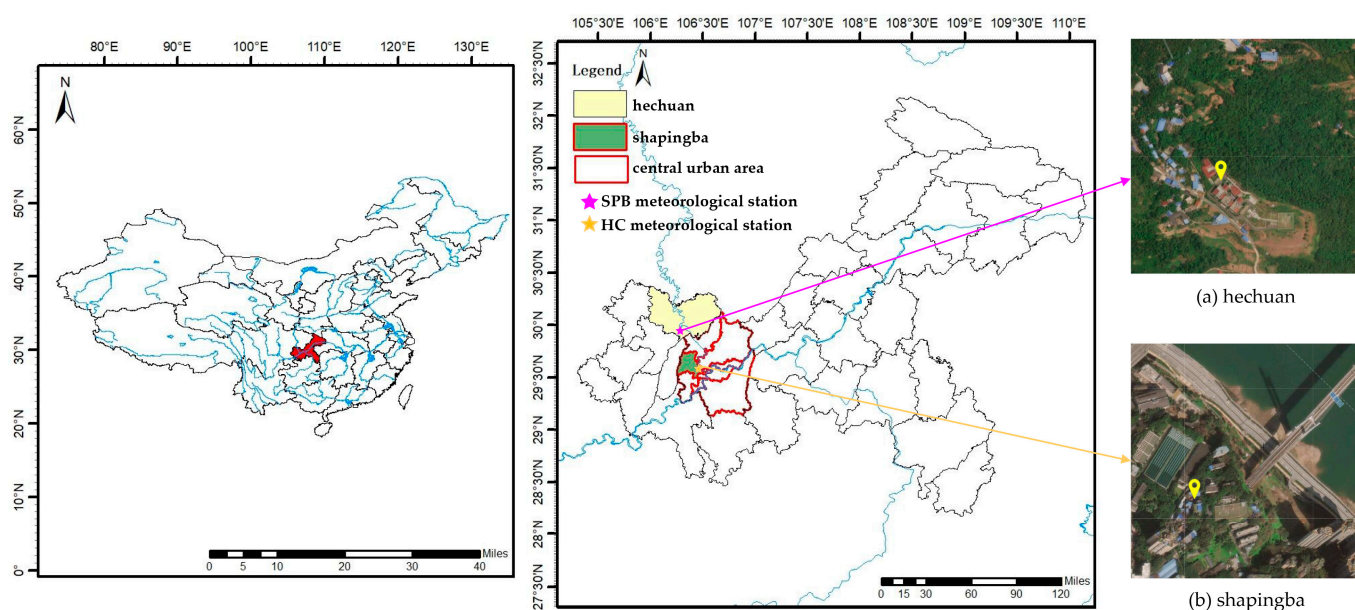


Figure 1. Location in Chongqing and distribution of meteorological stations: (a) Hechuan meteorological station; (b) Shapingba meteorological station.

Table 1. Detailed information about the 2 meteorological stations.

Station Name	ID	Latitude	Longitude	Elevation (m)	Frequency	Description
Shapingba	57516	29°35' N	106°28' E	259.1	3-Hour	urban (LCZ5)
Hechuan	57512	29°58' N	106°16' E	230.6		rural (LCZ9)

During the study period from 1959 to 2018, Chongqing experienced considerable urbanization. The urban population proportion of Chongqing increased from 31% to 65.5% from 1997 when it became a municipality directly under the central government to 2018 [31], the urban population and urbanization rate of Chongqing have been increasing steadily (Figure 2a,b). Chongqing's economy has also developed rapidly (Figure 2c). Therefore, considering the population and economic development of Chongqing, four indicators are selected to study the relationship between UHI and urbanization development, including urban resident population, gross domestic product (GDP), fixed investments, and gross industrial output value. These data were obtained from the Chongqing Statistical Yearbook and the Chinese City Statistical Yearbook during the past 20 years. In this paper, March–April–May is spring, June–July–August is summer, September–October–November is autumn, and December–January–February is winter.

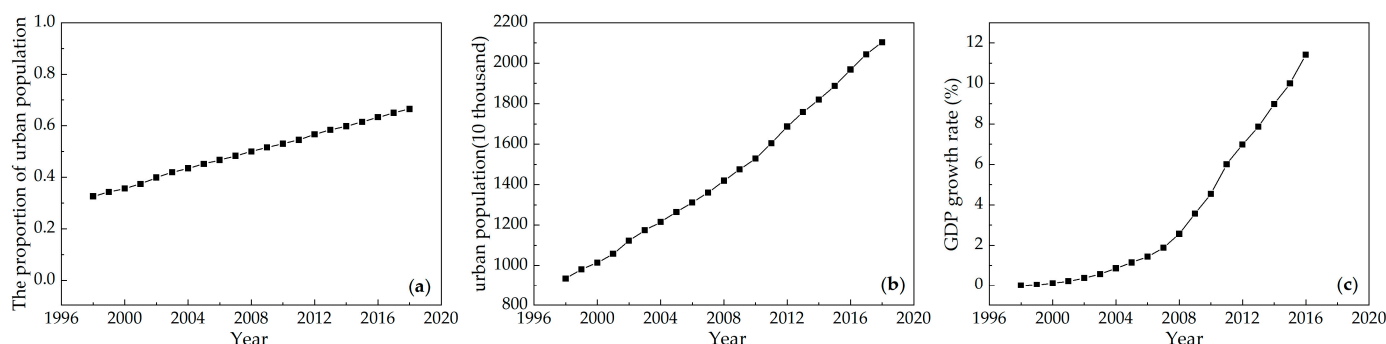


Figure 2. (a) The proportion of urban population in Chongqing; (b) urban population in Chongqing; (c) GDP growth rate from 1998 to 2016 (source: Chongqing Statistical Yearbook). Data for each year are indicated with black dots.

2.2. Methods

The study of the daily mean temperature for the period 1959–2018 from the two meteorological stations mentioned above aims to investigate possible trends in local climate and to determine the magnitude of the UHI effect, which can be done on an annual and seasonal basis. Daily maximum temperature and daily minimum temperature from the two meteorological stations are also used to better highlight the climatic characteristics of urban and rural areas. In this paper, the temperatures (mean, maximum, and minimum) of Shapingba station represent those of Chongqing's urban areas, and temperatures (mean, maximum and minimum) of Hechuan station represent those of Chongqing's rural areas. This paper uses the lapse rate of temperature to correct the temperature in rural areas to reduce the error caused by the altitude of meteorological stations. The lapse rate of temperature is $0.57\text{ }^{\circ}\text{C}/100\text{ m}$ during the day and $0.4\text{ }^{\circ}\text{C}/100\text{ m}$ at night [32].

The interannual and seasonal variation trends in temperatures (slopes) are calculated using the least-squares method. The Mann–Kendall test is used to determine the year in which this trend becomes statistically significant. The magnitude of the UHI effect can be expressed in terms of urban heat island intensity (UHII), which is the temperature difference between urban and rural areas in this paper. The grey relational analysis and the principal component analysis investigate the relationship between UHI and urbanization development. These methods are described in detail as follows:

1. Mann–Kendall test

The nonparametric test is the most common test to determine the temporal variation on meteorological variables [33]. The Mann–Kendall test is the most popular nonparametric statistical method for mutation detection and trend analysis [34,35]. It does not need samples to follow a certain distribution and is not disturbed by missing values and outliers [36]. This test can define the increasing or decreasing trends over the study period and the periods in which trends become statistically significant [37,38]. The Mann–Kendall test is calculated as follows:

x is used to represent a time series with a sample size of n . A rank series s_k is established as follows:

$$s_k = \sum_{i=1}^k r_i \quad k = 1, 2, \dots, n \tag{1}$$

$$r_i = \begin{cases} +1 & x_i > x_j \\ 0 & x_i \leq x_j \end{cases} \quad j = 1, 2, \dots, i \tag{2}$$

s_k is the cumulative value when the value at the time i is greater than the value at time j . In cases where the sample size $n > 10$, the standard normal test statistic UF_k is computed using Equation (3):

$$UF_k = \frac{[s_k - E(s_k)]}{\sqrt{var(s_k)}} \quad k = 1, 2, \dots, n \tag{3}$$

In the formula, $UF_1 = 0$, $E(s_k)$ and $var(s_k)$ are the mean value and variance of s_k , respectively. Positive values of UF_k indicate increasing trends, while negative UF_k values show decreasing trends. Testing trends is done at the specific α significance level. When $|UF_k| > Z_{1-\alpha/2}$, the null hypothesis is rejected, and a significant trend exists in the time series. $Z_{1-\alpha/2}$ is the standard normal variance, which can be obtained from the standard normal distribution table. In this paper, the significance level $\alpha = 0.05$ is used. In the two-tailed check, the null hypothesis for $\alpha = 0.05$ is rejected if $|UF_k| > 1.96$. Therefore, the trend becomes statistically significant if $|UF_k| > 1.96$.

Generate the corresponding inverse series x_n, x_{n-1}, \dots, x_1 from the time series x , repeat the above calculation process, and calculate UB_k using Equation (4):

$$UB_k = -UF_k \quad k = n, n - 1, \dots, 1 \tag{4}$$

In the formula, $UB_1 = 0$. If the intersection of UF_k and UB_k is located within the confidence interval, the corresponding time is the beginning time of the abrupt change in the series.

2. Calculation method of UHII

Take the difference in temperature between T_{urban} and T_{rural} as the UHII:

$$UHII_{mean} = (T_{mean,urban} - T_{mean,rural}) \tag{5}$$

$$UHII_{max} = (T_{max,urban} - T_{max,rural}) \tag{6}$$

$$UHII_{min} = (T_{min,urban} - T_{min,rural}) \tag{7}$$

As stated above, the interannual and seasonal of $UHII_{mean}$, $UHII_{max}$, and $UHII_{min}$ are calculated during the study period. In this study, $UHII_{max}$ and $UHII_{min}$ are also referred to as daytime UHII and nighttime UHII.

3. Grey relational analysis (GRA)

GRA is a method to solve the interrelationships between multiple factors [39]. In this paper, GRA was used to analyze the degree of correlation between urbanization factors

and UHII. The data of GRA need to be preprocessed because the scope and units of one data set may be different from the other [40]. The results are normalized by Equation (8):

$$x_i(j) = \frac{X_i(j)}{X_i(1)} \quad i = 1, 2, \dots, m \quad j = 1, 2, \dots, n \quad (8)$$

where $x_i(j)$ is normalized data, $i (1, 2, \dots, m)$ is the number of factors, and $j (1, 2, \dots, n)$ is the dimension of factors; the grey relational coefficient (GRC) is calculated from the normalized data obtained from Equation (9):

$$\xi_i(j) = \frac{\min_i \min_j |x_0(j) - x_i(j)| + \rho \max_i \max_j |x_0(j) - x_i(j)|}{|x_0(j) - x_i(j)| + \rho \max_i \max_j |x_0(j) - x_i(j)|} \quad (9)$$

where $x_0(j)$ denotes the reference sequence and $x_i(j)$ denotes the comparison sequence. In this paper, x_0 is UHII ($UHII_{mean}$, $UHII_{max}$, $UHII_{min}$), x_i is the four urbanization factors and j is the year. ρ is the distinguishing coefficient between 0 and 1. In this paper, $\rho = 1$. The grey relational grade (GRG) is computed by averaging the GRC by Equation (10):

$$r_i = \frac{1}{n} \sum_{j=1}^n \xi_i(j) \quad (10)$$

4. Principal component analysis (PCA)

PCA is a statistical method that applies an orthogonal transformation to convert a set of correlated variables into linearly uncorrelated variables [41,42]. By reducing the dimensions of the original variables, comprehensive indicators that affect the target variables are found. In this paper, SPSS software was used for PCA. The comprehensive urbanization index was calculated to represent the urbanization level of Chongqing. Moreover, the correlation analysis was carried out to establish a regression model between the comprehensive urbanization index and the UHII. Besides the urban resident population, three indicators related to the economic development of Chongqing are selected, including gross domestic product (GDP), fixed investments, and gross industrial output value.

The conceptual methodological flowchart in this paper is shown in Figure 3.

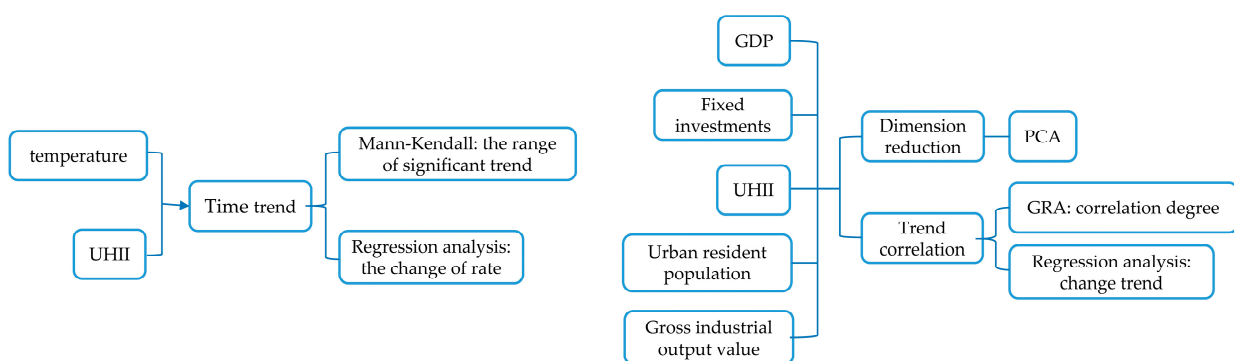


Figure 3. The conceptual methodological flowchart.

3. Results

3.1. Temporal Dynamics of Temperature Change in Chongqing

3.1.1. The Interannual Variation of Temperature

According to IPCC (2021), the global average temperature has increased by 1.1 °C. from 1850 to 2021 [43]. The rising trend of temperature is one of the main indicators of global warming and climate change. Over the past 100 years, the average temperature change trend in China is similar to that of the whole world, showing two significant

warming periods: the first in the 1920s–1940s, and the second after the 1980s [14,44]. In addition, studies have shown [44] that the annual mean temperature in China in the past 100 years has generally risen by $(0.78 \pm 0.27) ^\circ\text{C}$.

Figure 4 shows the time series of annual mean temperature, annual mean daily maximum temperature, and annual mean daily minimum temperature in urban and rural areas during the past 60 years (1959–2018). Our results indicate that the annual mean temperature for urban and rural areas (see Figure 4a) shows a downward trend from 1959 to the 1980s and an upward trend after the 1980s, which is practically consistent with the general temperature change trend of China [14,44]. Since our attention is given to the warming trend of Chongqing with urbanization, we focus on the linear trend rates and the statistical significance of the mean yearly temperature, mean annual daily maximum, and minimum temperature in urban and rural areas from 1985 to 2018. The warming trend is significantly weaker in rural areas than in urban areas ($4 ^\circ\text{C}/\text{century}$ in urban areas compared to $2.7 ^\circ\text{C}/\text{century}$ in rural areas). In comparison, the warming rates in the urban areas of Beijing and Wuhan are about $4.7 ^\circ\text{C}/\text{century}$ and $3.4 ^\circ\text{C}/\text{century}$, respectively [45]. Extreme temperature changes are more important than changes in the mean value because they are more relevant to local climate changes [37]; the changes in annual mean daily maximum temperature and annual mean daily minimum temperature are also recorded in this paper (see Figure 4b,c). The annual mean daily maximum and annual mean daily minimum temperature trends are $4.9 ^\circ\text{C}/\text{century}$ and $3.8 ^\circ\text{C}/\text{century}$ in urban areas, respectively, which are much higher than those in rural areas ($3.1 ^\circ\text{C}/\text{century}$ and $2.8 ^\circ\text{C}/\text{century}$, respectively). The difference between the annual mean daily minimum temperature in urban and rural areas remains large after 1973 (about $1 ^\circ\text{C}$), while the difference between the annual mean daily maximum temperature is relatively small. In other words, the daytime temperature of urban areas in Chongqing has been similar to that in rural areas over the past 60 years. However, urban areas are experiencing warmer nights than rural areas.

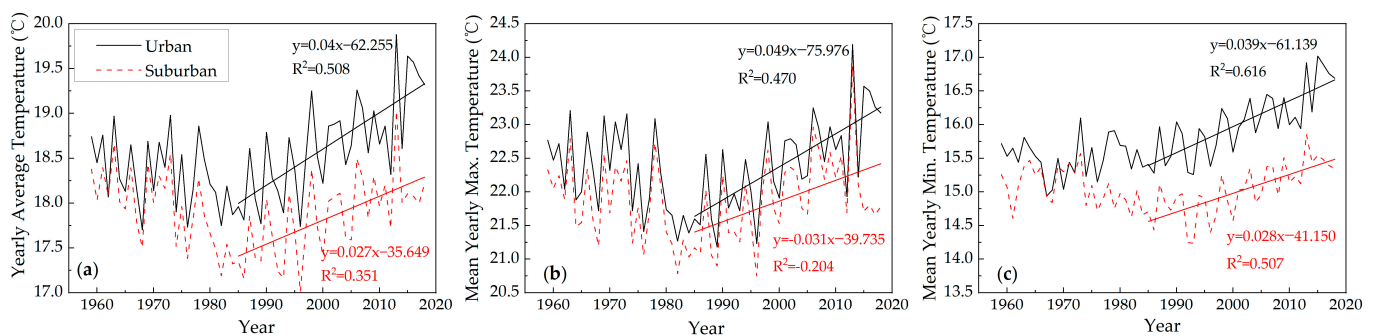


Figure 4. Temperature for urban and rural areas, 1959–2018: (a) yearly average temperature; (b) mean annual daily maximum temperature; (c) mean annual daily minimum temperature.

To exclude the effect of extreme values, the Mann–Kendall test is also used to examine the trends of temperature in urban and rural areas. Positive trends in annual mean temperature and annual mean daily minimum in urban areas are statistically significant in 2013 and 2003 onwards, respectively, with the abrupt changes in 2006 and 2002, respectively (see Figure 5a,e). However, the annual mean daily maximum temperature in urban areas is not significant, although a positive trend emerges after 2010. This indicates that the influence of urbanization is greater than that on the annual mean daily maximum temperature. In addition, the rising trends of temperature in rural areas are not statistically significant. Notably, the abrupt change points in both urban and rural areas after 2000 correspond to the rapid increase in Chongqing’s GDP in the 21st century. These findings may indicate that urbanization has a significant impact on the warming trend in Chongqing, and the

response rate is annual mean daily minimum temperature > annual mean temperature > annual mean daily maximum temperature.

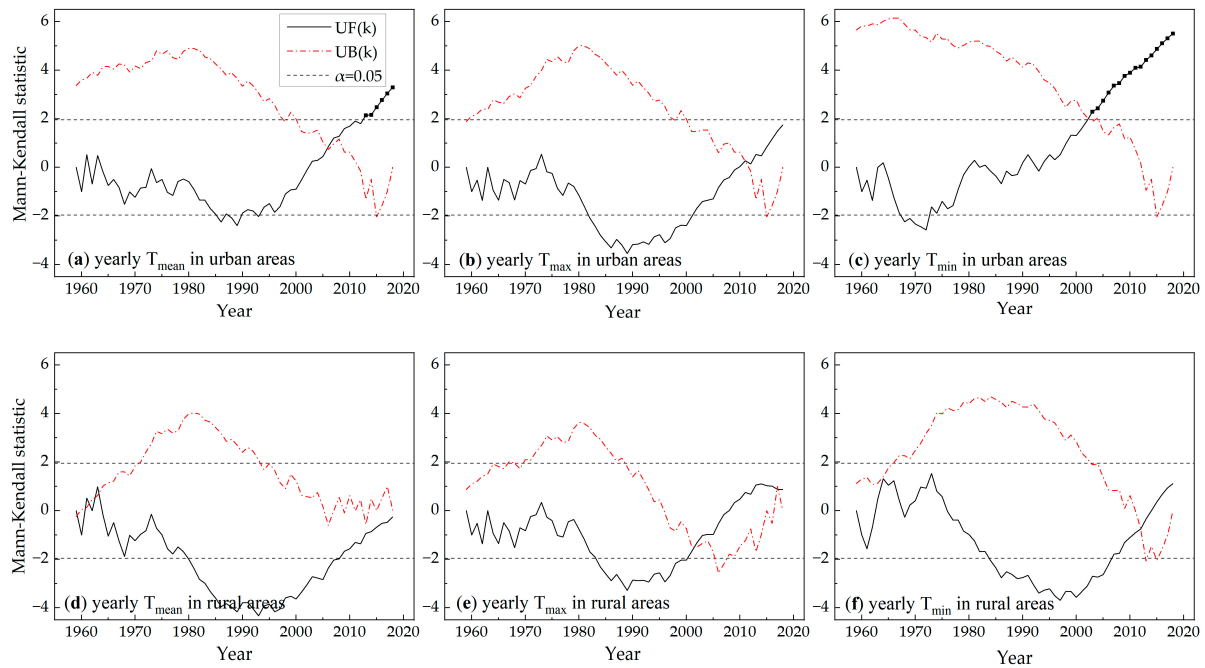


Figure 5. The Mann–Kendall statistic curves during the period of 1959–2018: (a) mean yearly temperature in urban areas; (b) mean yearly temperature in rural areas; (c) mean annual daily maximum temperature in urban areas; (d) mean annual daily maximum temperature in rural areas; (e) mean annual daily minimum temperature in urban areas; (f) mean annual daily minimum temperature in rural areas, and the period where the tendency is statistically significant UF(k) values higher than the limit of 1.96 at the significance level $\alpha = 0.05$ indicated with black dots.

3.1.2. The Seasonal Variation of Temperature

Table 2 shows the interannual and seasonal linear trend rates of the annual mean temperature, annual mean daily maximum temperature and annual mean daily minimum temperature in urban and rural areas from 1985 to 2018.

Table 2. The tendency rate of mean temperature, mean maximum and minimum temperature for urban and rural areas, 1985–2018.

	Tendency Rate (°C/Century)				
	Annual	Spring	Summer	Autumn	Winter
Mean temperature (urban)	4 **	5.5 **	5.6 **	3.2 **	1.9
Mean temperature (rural)	2.7 **	3.9 **	4.7 **	1.6	0.9
Mean maximum temperature (urban)	4.9 **	7.7 **	6.4 **	3.0	2.5
Mean maximum temperature (rural)	3.1 **	5.9 **	4.3 **	0.8	1.3
Mean minimum temperature (urban)	3.9 **	4.3 **	5.0 **	4.4 **	1.8
Mean minimum temperature (rural)	2.8 **	3.7 **	4.4 **	2.7	0.4

Note: ** indicates significance at $p < 0.01$; n.s.—nonsignificant.

By analyzing the mean temperature in urban and rural areas for each season separately, it is found that the mean temperature in spring and summer from 1985 to 2018 shows a statistically positive trend. Except for the annual mean daily minimum temperature in urban areas in autumn and the annual mean temperature, which show a statistically

significant increasing trend, the temperature trends in autumn and winter are not statistically significant. Meanwhile, spring and summer contribute more to the rising trends of temperature in urban and rural areas, whereas autumn and winter are relatively smaller. Wang et al. [46] found that the temperature varied more in summer, followed by spring and autumn, and least in winter by comparing surface temperatures in Chongqing in 2010 and 2020, which is consistent with the results of this paper.

Using the Mann–Kendall test, a statistically significant warming trend of mean temperature in urban areas appears only in autumn after 2010 (see Figure 6a). As for the analysis of the mean daily maximum temperature in urban areas for each season, no statistically significant positive trend is found, while the mean daily minimum temperature in urban areas shows a statistically significant warming trend in all seasons (see Figure 6b–e). As in the interannual analysis, the trends of the mean daily minimum temperature in urban areas for all seasons became statistically significant in a given year after 2000, indicating that the rapid urbanization development in Chongqing in the 21st century has had a significant impact on urban nighttime temperature. Although the linear trends of the mean daily maximum temperature in both urban and rural areas are large, they do not show significant trends in the Mann–Kendall test, suggesting that their linear rates of change may be due to abrupt temperature increases in individual years, but the overall trends are not statistically significant. In addition, the Mann–Kendall test in rural areas for each season does not show a positive statistically significant trend and thus is not included in Figure 6.

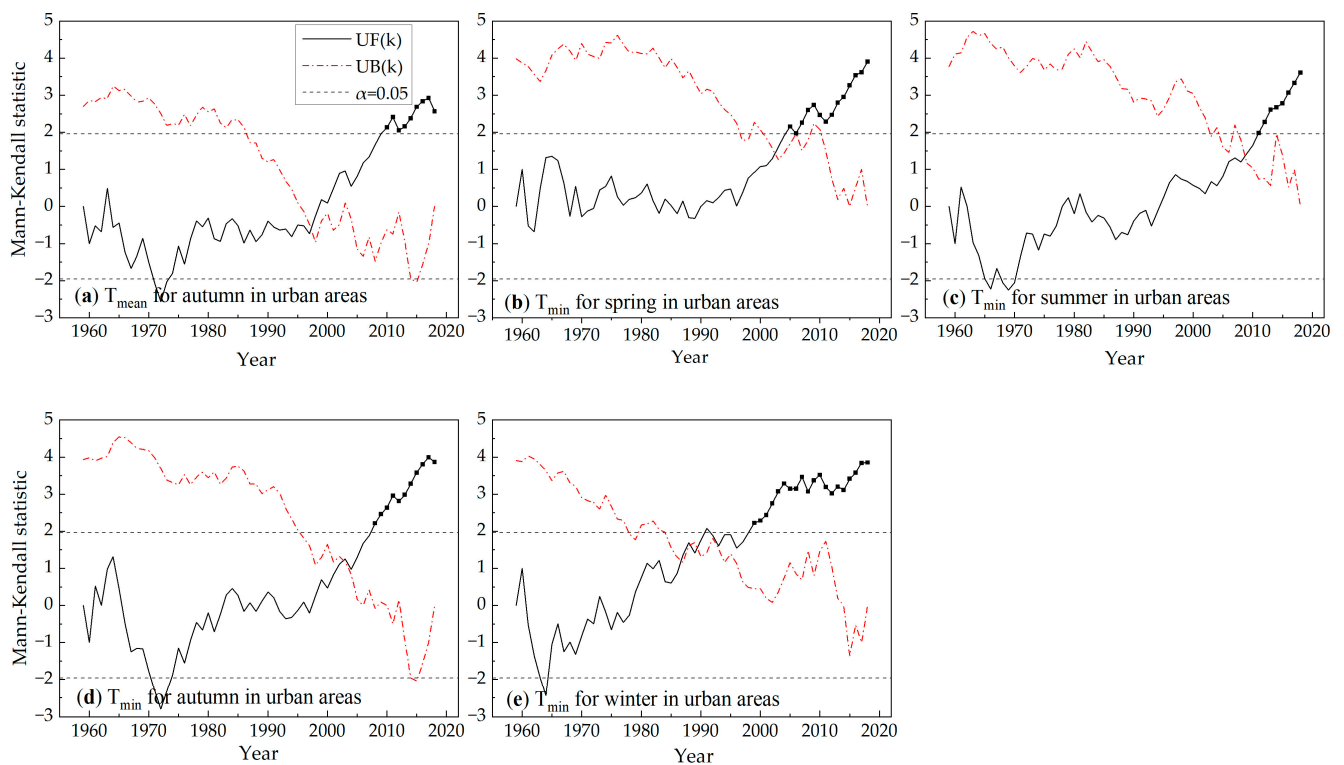


Figure 6. The Mann–Kendall statistic curves during the period of 1959–2018: (a) mean temperature for autumn in urban areas; (b) mean daily minimum temperature for spring in urban areas; (c) mean daily minimum temperature for summer in urban areas; (d) mean daily minimum temperature for autumn in urban areas; (e) mean daily minimum temperature for winter in urban areas.

3.2. Temporal Dynamics of UHI in Chongqing

3.2.1. The Inter-Annual Variation of UHII

As described in Section 3.1.1, the annual mean temperature warming rate of Chongqing urban areas during the last 60 years is much higher than that of rural areas. The feature is more clearly reflected by the interannual variation and trend of the $UHII_{mean}$ (see

Figure 7a). The annual $UHII_{mean}$ is progressive, indicating probably the ongoing urbanization of Chongqing. The growth trend of the annual $UHII_{mean}$ during the study period is about $1.4\text{ }^{\circ}\text{C}/\text{century}$. Before the 1970s, the annual $UHII_{mean}$ remained around $0.1\text{--}0.3\text{ }^{\circ}\text{C}$. With the rapid economic growth and industrialization at the end of the 20th century, Chongqing’s energy consumption and artificial heat emission increased sharply, leading to an upward trend in annual $UHII_{mean}$. Since then, the annual $UHII_{mean}$ has remained around $0.6\text{--}0.9\text{ }^{\circ}\text{C}$, reaching around $1.5\text{ }^{\circ}\text{C}$ after 2015. Liao et al. [26] pointed out that $UHII_{mean}$ in Chongqing from 2009–2018 was about $1\text{ }^{\circ}\text{C}$, which is close to the results of this paper. Considering that $UHII$ based on average temperature can mask the special characteristics of $UHII_{max}$ and $UHII_{min}$ [47], the interannual variation of the $UHII_{max}$ and $UHII_{min}$ are also analyzed. The annual $UHII_{min}$ increases by $1.7\text{ }^{\circ}\text{C}/\text{century}$ (see Figure 7c), while the rising trend of $UHII_{max}$ is much lower than that of $UHII_{mean}$ and $UHII_{min}$ and is not statistically significant (see Figure 7b). $UHII$ is weaker during the day and stronger at night, which is consistent with the conclusions of most scholars in the past. This may be related to the turbulent exchange in the near-surface layer [48]. In addition, $UHII$ rose abruptly due to the sharp warming in urban areas in 2015. Liao et al. [26] found a sharp expansion in the area of strong UHI in western Chongqing in recent years, which may indicate that drastic warming did occur in urban areas in western Chongqing. $UHII_{max}$, as the daytime extreme temperature difference between urban and rural areas, demonstrates more significant variation.

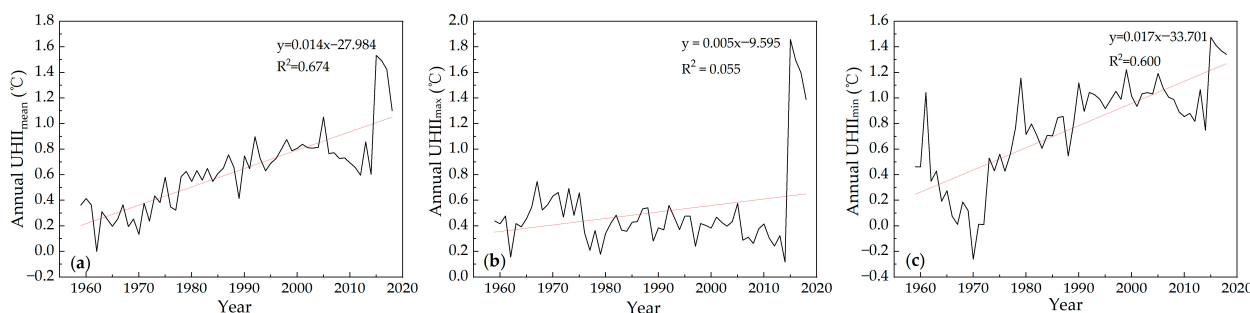


Figure 7. The interannual variation and trend, 1959–2018: (a) $UHII_{mean}$; (b) $UHII_{max}$; (c) $UHII_{min}$.

Using the Mann–Kendall test, the positive trends of $UHII_{mean}$ and $UHII_{min}$ are statistically significant after the 1980s, with no mutation points observed (see Figure 8a,c). This confirms that $UHII$ in Chongqing is progressive with the urbanization process. The annual $UHII_{max}$ is not statistically significant and even shows a decreasing trend after 1980 (see Figure 8b). This suggests that the slight growth rate of the annual $UHII_{max}$ obtained by the least-squares method may be due to its sharp increase in 2015, but its upward trend does not actually exist. These findings indicate that urbanization has a significant effect on $UHII_{mean}$ and $UHII_{min}$ in Chongqing, but not on $UHII_{max}$.

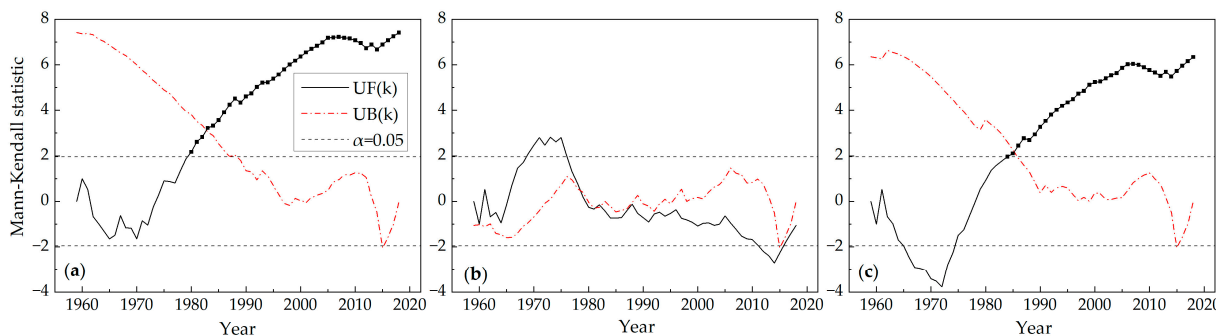


Figure 8. The Mann–Kendall statistic curves during the period of 1959–2018: (a) the annual $UHII_{mean}$; (b) the annual $UHII_{max}$; (c) the annual $UHII_{min}$.

3.2.2. The Seasonal Variation of UHII

The temporal variability of $UHII_{mean}$, daytime UHII, and nighttime UHII in Chongqing from 1959 to 2018 are calculated in Table 3. It can be seen that the rising trends of daytime UHII are not significant, while the trends of $UHII_{mean}$ and nighttime UHII are statistically significant ($p < 0.01$). As shown in Table 3, the increasing rate of $UHII_{mean}$ is greater in summer ($1.6\text{ }^{\circ}\text{C}/\text{century}$) and weaker in winter ($1.3\text{ }^{\circ}\text{C}/\text{century}$), which is similar to the results of the previous study in Chongqing [25] but different from those of other large cities in China. For example, Zhang et al. [49] found that the $UHII_{mean}$ of Shanghai is higher in autumn and weaker in summer. Li et al. [14] found that the $UHII_{mean}$ of Lanzhou in winter is highest. The $UHII_{mean}$ in Beijing is greater in winter and weaker in summer [50]. This may be attributed to higher summer temperature and increased anthropogenic heat release in the Sichuan basin, while there is no heating energy demand in winter. The increasing rates of $UHII_{mean}$ in spring and summer exceed the annual increasing rate. In addition, the growth rate of $UHII_{min}$ is greater in autumn ($1.7\text{ }^{\circ}\text{C}/\text{century}$), followed by summer and winter ($1.6\text{ }^{\circ}\text{C}/\text{century}$), and weaker in spring ($1.4\text{ }^{\circ}\text{C}/\text{century}$), while $UHII_{max}$ is greater in winter and spring.

Table 3. The tendency rate and statistically significant of $UHII_{mean}$, $UHII_{max}$ and $UHII_{min}$ during the period of 1959–2018.

	Tendency Rate ($^{\circ}\text{C}/\text{Century}$)				
	Annual	Spring	Summer	Autumn	Winter
$UHII_{mean}$	1.4 **	1.5 **	1.6 **	1.4 **	1.3 **
$UHII_{max}$ (daytime UHII)	0.5	0.7	0.3	0.4	0.7
$UHII_{min}$ (nighttime UHII)	1.7 **	1.4 **	1.6 **	1.7 **	1.6 **

Note: ** indicates significance at $p < 0.01$; n.s.—nonsignificant.

The analysis of $UHII_{mean}$ and nighttime UHII shows a statistically significant upward trend for all seasons after the 1980s using the Mann–Kendall test (see Figure 9). No mutations exist except for the summer $UHII_{mean}$ in 1981. It further verifies that since the Chinese reform process began in the late 1970s, UHII has been increasing gradually and progressively with the urbanization process in Chongqing, and it is more sensitive to urbanization factors than temperature. Additionally, $UHII_{max}$ for each season does not show statistical significance according to the Mann–Kendall test and therefore is not shown in Figure 10.

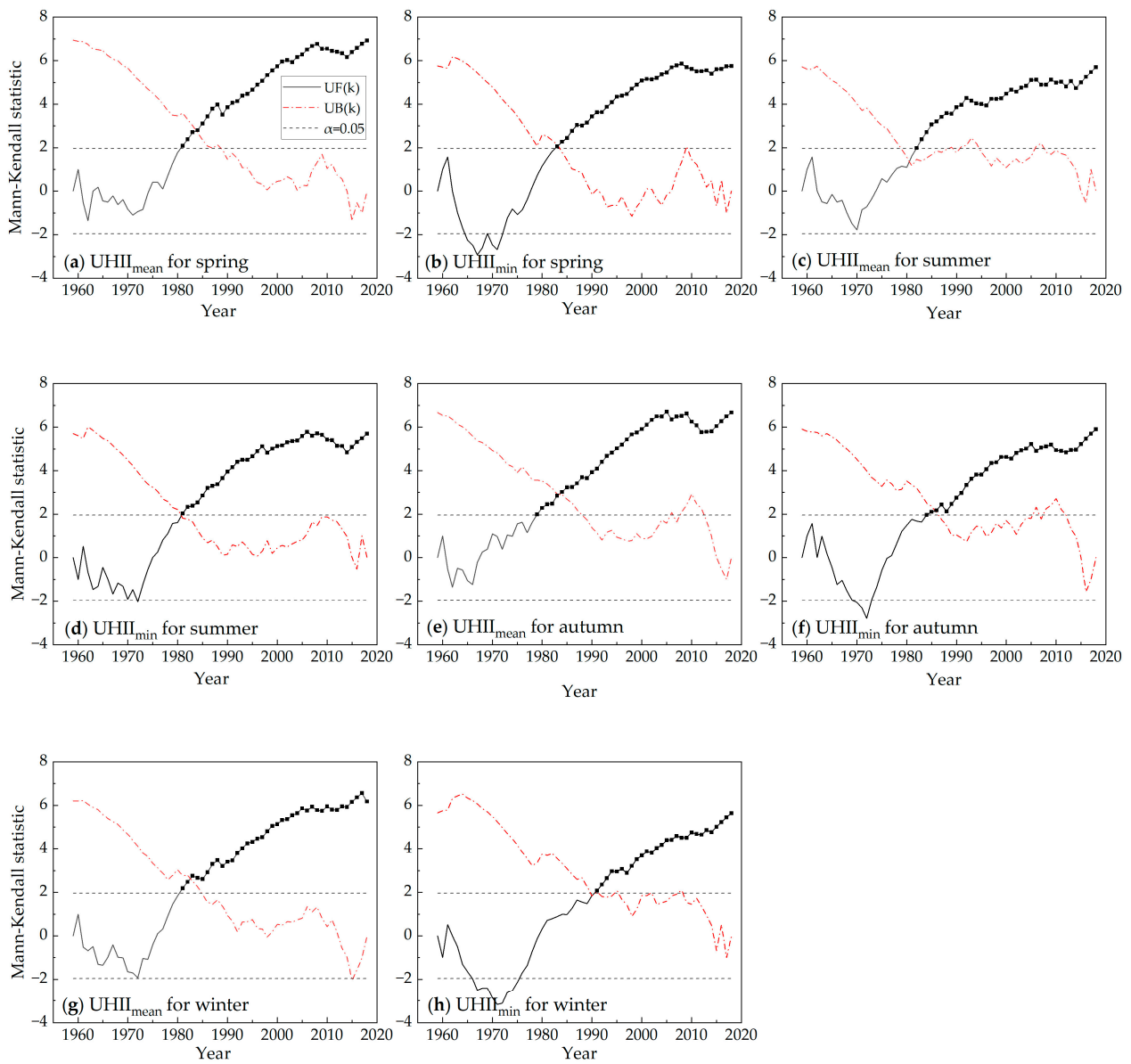


Figure 9. The Mann–Kendall statistic curves during the period of 1959–2018: (a) UHII_{mean} for spring; (b) UHII_{min} for spring; (c) UHII_{mean} for summer; (d) UHII_{min} for summer; (e) UHII_{mean} for autumn; (f) UHII_{min} for autumn; (g) UHII_{mean} for winter; (h) UHII_{min} for winter.

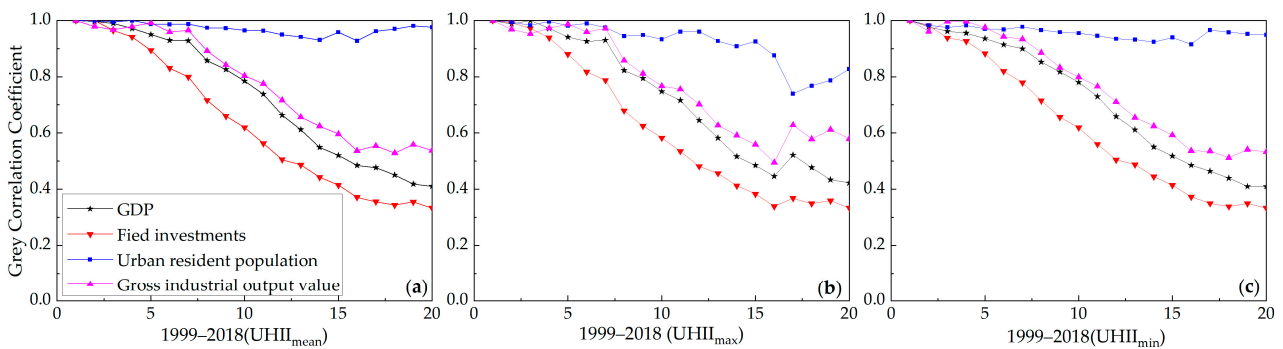


Figure 10. GRA of between the urbanization factors and UHII in Chongqing: (a) UHII_{mean}; (b) UHII_{max}; (c) UHII_{min}.

3.3. Quantitative Analysis between the Urbanization Factors and UHI

3.3.1. GRA of between the Urbanization Factors and UHII

Using GRA, we can know which other factors are related to UHII (UHII_{mean}, UHII_{max}, UHII_{min}). Urban population refers to the number of residents living in urban areas, which can be used as an alternative indicator of urban physical structure [51]. Urban economics-related data are important indicators of urban economic aggregate and development, which are related to energy consumption, industrial development and commercial land expansion. According to a previous study [14], the three most relevant factors for economic development are selected: GDP, fixed investment and gross industrial output value. The UHII in Chongqing from 1999 to 2018 is used as the reference sequence. GDP, fixed investments, urban resident population, and gross industrial output value are used as the comparison sequence to conduct GRA by MATLAB R2020b. The GRC and GRG between GDP, fixed investments, urban resident population, gross industrial output value and UHII are shown in Figure 11 and Table 4. The GRG between urban resident population and UHII_{mean}, UHII_{max}, and UHII_{min} are 0.971, 0.921, and 0.957, respectively, with the largest positive correlation. The GRG of GDP, fixed investments, gross industrial output value, and UHII (UHII_{mean}, UHII_{max}, UHII_{min}) are all greater than 0.5. Therefore, it is concluded that UHII is related to these four indicators and is more related to urban population factors than to urban economics factors. In the following section, we will quantitatively analyze the relationship between the urbanization factors and UHII.

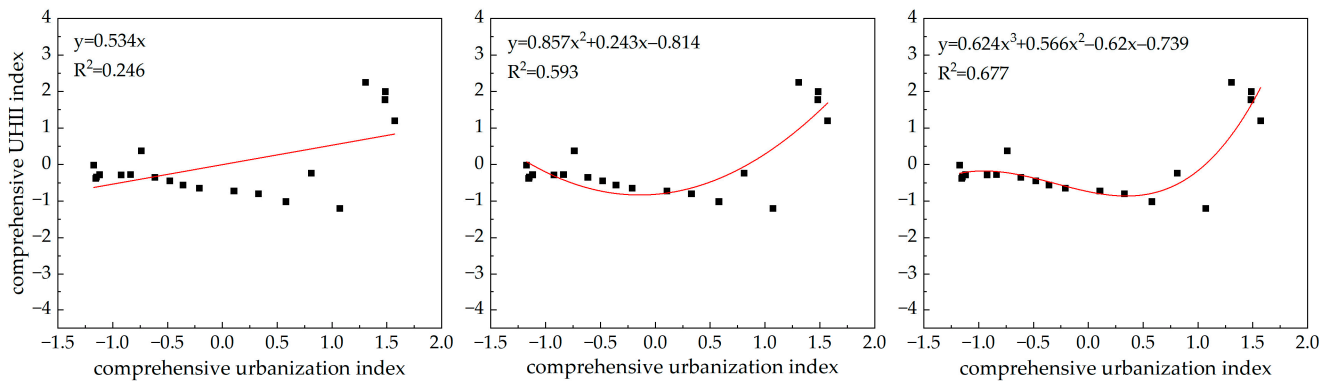


Figure 11. Relationship between comprehensive UHII index and the comprehensive urbanization index in Chongqing. Data for each year are indicated with black dots.

Table 4. GRG of between the urbanization factors and UHII in Chongqing.

Station Name	GRG			
	GDP	Fixed Investments	Urban Resident Population	Gross Industrial Output Value
UHII _{mean}	0.728	0.630	0.971	0.773
UHII _{max}	0.718	0.615	0.921	0.769
UHII _{min}	0.718	0.624	0.957	0.766

3.3.2. The Quantitative Relationship between the Urbanization Factors and UHII

The above indicators are selected for principal component analysis to study the relationship between UHI and urban development quantitatively. The correlation analysis between the variables shows that they are highly correlated (see Tables 5 and 6), so PCA can be effectively used for dimension reduction.

Table 5. Correlation matrix of UHII (UHII_{mean}, UHII_{max}, UHII_{min}).

	UHII _{max}	UHII _{min}	UHII _{mean}
UHII _{max}	1 **	0.877 **	0.961 **
UHII _{min}	0.877 **	1 **	0.918 **
UHII _{mean}	0.961 **	0.918 **	1 **

Note: ** indicates significance at $p < 0.01$; n.s.—nonsignificant.

Table 6. Correlation matrix of urbanization factors.

	GDP	Fixed Investments	Urban Resident Population	Gross Industrial Output Value
GDP	1 **	0.988 **	0.948 **	0.984 **
Fixed investments	0.988 **	1 **	0.973 **	0.995 **
Urban resident population	0.948 **	0.973**	1 **	0.96 **
Gross industrial output value	0.984 **	0.995 **	0.96 **	1 **

Note: ** indicates significance at $p < 0.01$; n.s.—nonsignificant.

The standardization of standard deviation is used to process the data by SPSS. The results are shown in Table 7. Usually, the cumulative variance contribution rate is not lower than 85% to determine the number of principal components [52]. The results show that the cumulative variance contribution rates of the first item for urbanization factors and UHII are 98.098% and 94.567%, respectively (see Table 8). Therefore, the first principal component can reflect urban development level and UHII. By the principal component score coefficient matrix Z1, the principal component scores calculated by the factor loads corresponding to the first principal component can be used as the urban development index and the UHII index, and their equations are as follows:

$$x = 0.254FI + 0.252GDP + 0.25URP + 0.253GIOV \tag{11}$$

$$y = 0.348UHII_{mean} + 0.343UHII_{max} + 0.337UHII_{min} \tag{12}$$

Table 7. Index characteristic values and contribution rates.

	Principal Component	Eigenvalue	Contribution Rate (%)	Accumulation Rate (%)
Urbanization factors	1	3.924	98.098	98.098
	2	0.058	1.449	99.547
	3	0.015	0.277	99.924
	4	0.003	0.076	100.000
UHII (UHII _{mean} , UHII _{max} , UHII _{min})	1	2.837	94.567	94.567
	2	0.130	4.330	98.897
	3	0.033	1.103	100.000

Table 8. Component load matrix (F1) and score matrix (Z1).

		F1	Z1
Urbanization Indices	Fixed investments	0.998	0.254
	GDP	0.990	0.252
	Urban resident population	0.979	0.250
	Gross industrial output value	0.994	0.253
UHII	UHII _{mean}	0.987	0.348
	UHII _{max}	0.973	0.343
	UHII _{min}	0.957	0.337

By establishing the primary, secondary, and tertiary regression models between the urban development index and the UHII index, it is found that the tertiary regression model has the best fit with $R^2 = 0.677$ ($p < 0.01$) (see Figure 11). This suggests that there is not a simple linear relationship between the UHI and the urbanization factors. We can see that the UHII of Chongqing from 1999 to 2018 has been on a sharp upward trend after a slight decrease with the increase of urbanization index. While in the study of the northwest region, UHII has started to show a decreasing trend after reaching its peak in recent years, i.e., these cities have entered a coordinated development phase (Lanzhou [14], Xi'an, Yinchuan and Urumqi [53]). However, UHII in Chongqing will continue to increase rapidly with urban development, so effective urban eco-environmental construction strategies are still necessary and pressing.

4. Discussion

The long-term temperature variation trends and the UHI temporal dynamics variation characteristics of Chongqing are studied using the long-term observation data of urban and surrounding non-urban meteorological stations. In the study, the limited number of meteorological stations in urban and rural areas introduces some limitations. Furthermore, the locations of these meteorological stations are not dense enough to allow their historical data to reflect the spatial distribution of UHI in Chongqing. Fortunately, our study mainly focuses on the changes of UHI over time, so it is considered that the selection of these meteorological stations is appropriate.

The temperature in Chongqing can be divided into two periods over the past 60 years. It was the cold period before 1984 and then it started to get warmer, which is generally in line with the climate change trends in other parts of China [41]. Yao et al. [54] reported that the warming trend in Chongqing from 1951 to 2010 was $1.0\text{ }^\circ\text{C}/\text{century}$, but this value has reached $1.4\text{ }^\circ\text{C}/\text{century}$ (1959–2018) in our study. The warming rates are larger in spring and summer, and both exceed the annual mean warming rate, while those in autumn and winter are smaller. The rising trend of temperature in Chongqing urban areas may be the result of rapid urbanization, high population density, and other anthropogenic factors. According to Bao et al. [55], from 2009 to 2017, Chongqing became the fastest growing city in China with an average annual GDP growth rate of more than 14% and ranked fifth in GDP in 2017. Furthermore, the 'One Belt, One Road' initiative announced in 2013 has provided vast opportunities for the development of Chongqing. The development of the urban economy has led to an expansion in population and urbanization that may affect the long-term temperature of the city. Accordingly, the Mann–Kendall test shows that the rising trend of temperature in urban areas increased significantly during this period. The positive trend in annual mean temperature in urban areas is statistically significant after 2013, with the abrupt change starting in 2006. Meanwhile, the temperature and warming rates in rural areas are significantly lower than those in urban areas.

The growth trend of the annual $\text{UHII}_{\text{mean}}$ in Chongqing during the study period is about $1.4\text{ }^\circ\text{C}/\text{century}$. The annual $\text{UHII}_{\text{mean}}$ can reach up to $1.5\text{ }^\circ\text{C}$. Compared with other seasons, $\text{UHII}_{\text{mean}}$ in Chongqing is stronger in summer, at about $1.67\text{ }^\circ\text{C}$, and weaker in autumn and winter. Yao et al. [54] found that the maximum UHII in Chongqing can be as high as $2.5\text{ }^\circ\text{C}$ by numerical simulation, considering that UHII values vary in the same city depending on measurement time and methods, and also vary from city to city depending on the level of development and climatic conditions. The $\text{UHII}_{\text{mean}}$ in other regions are shown in Table 9. Although the time series of these studies are different, we can have an overview of the UHII in other regions. It also can be seen that the $\text{UHII}_{\text{mean}}$ in Chongqing is higher than that in other southern cities of China, but much lower than that in northern cities. Moreover, with the Chinese reform process and urbanization, the seasonal and interannual $\text{UHII}_{\text{mean}}$ and nighttime UHII show statistically significant and gradual increases after the 1980s (no abrupt change), which implies that urbanization has a greater effect on $\text{UHII}_{\text{mean}}$ and nighttime UHII, and UHII responds more rapidly to urbanization

than temperature. In addition, the reasons for the dramatic change in UHII in 2015 were not analyzed, which is a limitation of this study.

Table 9. Annual UHII_{mean} of several cities (°C).

City	Population	Annual UHII _{mean}
Beijing [56]	2188.6×10^4	1.81
Xi'an (Shaanxi Province) [57]	1316.30×10^4	1.47
Shanghai [58]	2489.43×10^4	0.99
Nanjing (Jiangsu Province) [48]	942.34×10^4	1.1
Seoul (Korea) [59]	949.69×10^4	1.3
Tokyo (Japan) [60]	1394.3×10^4	2.4

UHII is mainly related to weather conditions and urban morphology. Many studies showed the influence of weather conditions on UHII; it is higher in calm and clear weather, while lower or even disappears in cloudy and windy weather [61]. UHII is inversely proportional to cloud cover and wind speed [62,63]. However, this paper mainly studies the correlation between UHII and urbanization factors. Four indicators closely related to urbanization development and UHII are selected for PCA to form a comprehensive urbanization index and a comprehensive UHII index. The relationship between Urbanization Factors and UHII is analyzed; as shown in Figure 11, UHII in Chongqing is currently in a phase of rapid increase with urbanization factors. In the meantime, UHII reached a coordinated development stage in northwest China where it has declined with urbanization. However, the UHII in Chongqing has not yet reached its peak. Therefore, in Chongqing, we cannot assume for now that the UHI effect will be solved naturally with urban development; policy guidance and social intervention are very necessary.

Continued exposure to the effects of UHI could have serious impacts on the residents' health, urban economy, and social development. We can propose mitigation measures according to the urban characteristics and the changes of UHII in Chongqing, such as planning ventilation corridors, especially in riverside areas [64]; suitable tree species (e.g., camphor) can be selected to strengthen belt greening and extend to surrounding buildings to form three-dimensional greening [65,66]; accelerating the construction of the sponge city; adjusting the landscape water volume in each season [67]; and utilizing natural cold sources, such as the Jialing River and the Yangtze River [68,69].

5. Conclusions

Compared with other cities in China, Chongqing has a unique track of urbanization and economic growth, thus providing a unique opportunity to better understand the temporal variability of temperature and UHI. In this paper, the daily temperature data from two meteorological stations from 1959 to 2018 are analyzed to explore the interannual and seasonal variation characteristics of temperature and UHI in Chongqing using the least-squares method and the Mann–Kendall test. In addition, the quantitative relationship between urbanization factors and the UHI is studied using grey relational analysis and principal component analysis. The conclusions are as follows:

1. The temperatures in urban and rural areas of Chongqing show a noticeable increasing trend after 1985, and the warming rate in urban areas ($4\text{ }^\circ\text{C}/\text{century}$) is higher than that in rural areas ($2.7\text{ }^\circ\text{C}/\text{century}$) due to urbanization. During the study period, the warming rates are higher in spring and summer in urban and rural areas. Using the Mann–Kendall test, it is shown that with the rapid urbanization of Chongqing in the 21st century, the temperatures in urban and rural areas experienced abrupt changes during this period. The annual mean temperature and annual mean daily minimum temperature in urban areas show a statistically significant positive trend after 2013 and 2003, respectively. The mean daily minimum temperature for all seasons and the mean temperature in autumn in urban areas show a significant upward trend, while the temperature trends in rural areas are not significant.

2. The statistically significant upward trends of $UHII_{mean}$ and $UHII_{min}$ in Chongqing are progressive with urbanization. During the study period, UHII increased at most from 0.1 °C to 1.5 °C. The growth rate of $UHII_{mean}$ is stronger in summer (1.6 °C/century) and weaker in winter (1.3 °C/century). Whereas the growth rate of $UHII_{min}$ is stronger in autumn (1.7 °C/century) and weaker in spring (1.4 °C/century). The Mann–Kendall test for $UHII_{max}$ shows a non-significant decreasing trend, and the slightly increasing rate (0.5 °C/century) in the linear trend may be attributed to the sharp increase in temperature in urban areas of Chongqing in 2015. The nighttime UHII during the study period is much stronger than the daytime UHII in all seasons, and this difference is larger in summer and autumn.
3. $UHII_{mean}$, $UHII_{max}$, and $UHII_{min}$ are proved to be related to urbanization factors and more related to urban resident population using GRA. The comprehensive UHII index and the comprehensive urbanization index are constructed using PCA and a tertiary regression model is established. The curve obtained by the model shows that although the relationship between UHI and urbanization factors is not simply linear, and UHII in Chongqing is currently in a phase of rapid increase with urbanization factors. It is necessary to accelerate the implementation of effective urban ecological construction strategies.
4. The limited number of long-term meteorological stations in Chongqing introduces some limitations to this paper, and other methods can be used in the future to improve the comprehension of the changing characteristics of UHII in Chongqing. This paper explores the quantitative relationship between UHI and urbanization factors, but a comprehensive analysis of the reasons for the change in UHI with urbanization factors is not provided. Meanwhile, UHII is not only related to urbanization factors, but weather conditions also influence daily UHII. A more in-depth and detailed study can be conducted in the future, which will help to make targeted urban planning recommendations.

Author Contributions: All authors contributed equally in the preparation of this manuscript. Conceptualization, J.Z. and L.T.; methodology, L.T.; software, J.Z.; validation, J.Z.; formal analysis, L.T.; investigation, L.T.; data curation, J.Z.; writing—original draft preparation, J.Z. and L.T.; writing—review and editing, J.Z.; visualization, J.Z.; supervision, J.L.; project administration, J.L.; funding acquisition, J.L. All authors have read and agreed to the published version of the manuscript.

Funding: The study was sponsored by National Natural Science Foundation of China (No.51708054), Chengdu Science and Technology Project (No.2019-YF05-01377-SN), and the Fundamental Research Funds for the Central Universities (No.2018CDXYCH0015).

Institutional Review Board Statement: Not applicable.

Informed Consent Statement: Not applicable.

Data Availability Statement: Restrictions apply to the availability of these data. Data were obtained from the National Meteorological Information Center and are available [<http://data.cma.cn/>] (accessed on 2 September 2020) with the permission of the National Meteorological Information Center.

Acknowledgments: The authors thank the National Meteorological Information Center for providing past climate data of the study districts. We thank the anonymous reviewers and the editors of the journal for their constructive comments, suggestions, and edits to the manuscript.

Conflicts of Interest: The authors declare no conflict of interest.

References

1. Nations, U. Key Facts. In *World Urbanization Prospects 2018*; United Nations Publications: New York, NY, USA, 2018.
2. Yu, Z.; Yao, Y.; Yang, G.; Wang, X.; Vejre, H. Spatiotemporal patterns and characteristics of remotely sensed region heat islands during the rapid urbanization (1995–2015) of Southern China. *Sci. Total Environ.* **2019**, *674*, 242–254. [[CrossRef](#)]
3. Sun, R.; Lü, Y.; Yang, X.; Chen, L. Understanding the variability of urban heat islands from local background climate and urbanization. *J. Clean. Prod.* **2019**, *208*, 743–752. [[CrossRef](#)]

4. Yue, W.; Qiu, S.; Xu, H.; Xu, L.; Zhang, L. Polycentric urban development and urban thermal environment: A case of Hangzhou, China. *Landsc. Urban Plan.* **2019**, *189*, 58–70. [[CrossRef](#)]
5. Peng, S.; Feng, Z.; Liao, H.; Huang, B.; Peng, S.; Zhou, T. Spatial-temporal pattern of, and driving forces for, urban heat island in China. *Ecol. Indic.* **2019**, *96*, 127–132. [[CrossRef](#)]
6. Mirzaei, P.A.; Haghighat, F. Approaches to study Urban Heat Island—Abilities and limitations. *Build. Environ.* **2010**, *45*, 2192–2201. [[CrossRef](#)]
7. Xu, D.; Zhou, D. Research on the Planning Methods of Mitigating Summer Urban Heat Island Effects among Basin Cities—A Case Study at Xi’an, China. *Procedia Eng.* **2016**, *169*, 248–255. [[CrossRef](#)]
8. Min, M.; Lin, C.; Duan, X.; Jin, Z.; Zhang, L. Spatial distribution and driving force analysis of urban heat island effect based on raster data: A case study of the Nanjing metropolitan area, China. *Sustain. Cities Soc.* **2019**, *50*, 101637. [[CrossRef](#)]
9. Li, K.; Chen, Y.; Wang, M.; Gong, A. Spatial-temporal variations of surface urban heat island intensity induced by different definitions of rural extents in China. *Sci. Total Environ.* **2019**, *669*, 229–247. [[CrossRef](#)] [[PubMed](#)]
10. Streutker, D.R. Satellite-measured growth of the urban heat island of Houston, Texas. *Remote Sens. Environ.* **2003**, *85*, 282–289. [[CrossRef](#)]
11. Voogt, J.A.; Oke, T.R. Thermal remote sensing of urban climates. *Remote Sens. Environ.* **2003**, *86*, 370–384. [[CrossRef](#)]
12. Li, H.; Zhou, Y.; Wang, X.; Zhou, X.; Zhang, H.; Sodoudi, S. Quantifying urban heat island intensity and its physical mechanism using WRF/UCM. *Sci. Total Environ.* **2019**, *650*, 3110–3119. [[CrossRef](#)]
13. Antoniou, N.; Montazeri, H.; Neophytou, M.; Blocken, B. CFD simulation of urban microclimate: Validation using high-resolution field measurements. *Sci. Total Environ.* **2019**, *695*, 133743. [[CrossRef](#)]
14. Li, G.; Zhang, X.; Mirzaei, P.A.; Zhang, J.; Zhao, Z. Urban heat island effect of a typical valley city in China: Responds to the global warming and rapid urbanization. *Sustain. Cities Soc.* **2018**, *38*, 736–745. [[CrossRef](#)]
15. Liu, Y.; Xu, Y.; Weng, F.; Zhang, F.; Shu, W. Impacts of urban spatial layout and scale on local climate: A case study in Beijing. *Sustain. Cities Soc.* **2021**, *68*, 102767. [[CrossRef](#)]
16. Kedia, S.; Bhakare, S.P.; Dwivedi, A.K.; Islam, S.; Kaginalkar, A. Estimates of change in surface meteorology and urban heat island over northwest India: Impact of urbanization. *Urban Clim.* **2021**, *36*, 100782. [[CrossRef](#)]
17. Macintyre, H.L.; Heaviside, C.; Cai, X.; Phalkey, R. The winter urban heat island: Impacts on cold-related mortality in a highly urbanized European region for present and future climate. *Environ. Int.* **2021**, *154*, 106530. [[CrossRef](#)] [[PubMed](#)]
18. Yao, L.; Sun, S.; Song, C.; Li, J.; Xu, W.; Xu, Y. Understanding the spatiotemporal pattern of the urban heat island footprint in the context of urbanization, a case study in Beijing, China. *Appl. Geogr.* **2021**, *133*, 102496. [[CrossRef](#)]
19. Moazzam, M.F.U.; Doh, Y.H.; Lee, B.G. Impact of urbanization on land surface temperature and surface urban heat Island using optical remote sensing data: A case study of Jeju Island, Republic of Korea. *Build. Environ.* **2022**, *222*, 109368. [[CrossRef](#)]
20. Barrao, S.; Serrano-Notivoli, R.; Cuadrat, J.M.; Tejedor, E.; Sánchez, M.A.S. Characterization of the UHI in Zaragoza (Spain) using a quality-controlled hourly sensor-based urban climate network. *Urban Clim.* **2022**, *44*, 101207. [[CrossRef](#)]
21. Leconte, F.; Bouyer, J.; Claverie, R.; Pétrissans, M. Using Local Climate Zone scheme for UHI assessment: Evaluation of the method using mobile measurements. *Build. Environ.* **2015**, *83*, 39–49. [[CrossRef](#)]
22. Cao, Q.; Yu, D.; Georgescu, M.; Wu, J. Impacts of urbanization on summer climate in China: An assessment with coupled land-atmospheric modeling. *J. Geophys. Res. Atmos.* **2016**, *121*, 10505–10521. [[CrossRef](#)]
23. Cai, Z.; Liu, Z.; Zuo, S.; Cao, S. Finding a Peaceful Road to Urbanization in China. *Land Use Policy* **2019**, *83*, 560–563. [[CrossRef](#)]
24. Liu, C.; Li, Y. Spatio-Temporal Features of Urban Heat Island and Its Relationship with Land Use/Cover in Mountainous City: A Case Study in Chongqing. *Sustainability* **2018**, *10*, 1943. [[CrossRef](#)]
25. Jiang, P.; Liu, X.; Zhu, H.; Li, Y. Features of Urban Heat Island in Mountainous Chongqing from a Dense Surface Monitoring Network. *Atmosphere* **2019**, *10*, 67. [[CrossRef](#)]
26. Liao, D.; Zhu, H.; Jiang, P. Study of urban heat island index methods for urban agglomerations (hilly terrain) in Chongqing. *Theor. Appl. Climatol.* **2021**, *143*, 279–289. [[CrossRef](#)]
27. Liu, X.; Ming, Y.; Liu, Y.; Yue, W.; Han, G. Influences of landform and urban form factors on urban heat island: Comparative case study between Chengdu and Chongqing. *Sci. Total Environ.* **2022**, *820*, 153395. [[CrossRef](#)] [[PubMed](#)]
28. Yang, W.; Dan, Y.; Jie, M.; Feitong, Z.; Yu, W.; Xiaoqiao, W.; Hongrui, Z. Spatial pattern analysis and quantitative detection of multi-Factor influence for urban heat island effect in a mountainous city: A case study of Chongqing metropolitan circle. *Geogr. Res.* **2021**, *40*, 856–868.
29. Haonan, Z.; Xiaoran, L.; Jia, S.; Jie, Z.; Bingyan, C.; Ning, Z. Evaluation of the Urban Heat Island Effect of Sponge City in Chongqing using Satellite Remote Sensing Data and Numerical Simulation. *Plateau Meteorol.* **2021**, *40*, 1202–1212.
30. Karl, T.R.; Diaz, H.F.; Kukla, G. Urbanization: Its Detection and Effect in the United States Climate Record. *J. Clim.* **1988**, *1*, 1099–1123. [[CrossRef](#)]
31. Chongqing Municipal Bureau of Statistics; National Bureau of Statistics of China. *Chongqing Statistical Yearbook 2019*; China Statistics Press: Beijing, China, 2019.
32. Shang-ming, D.; Hai-feng, A.; Bo, N.D.A.; Hui-xi, X.; Ling, G.Y.A.N.; Gang-yi, N.C.H.E. An analysis of urban heat island effects in Chongqing based on AVHRR and DEM. *Resour. Environ. Yangtze Basin* **2009**, *7*, 680–685.
33. Güçlü, Y.S. Multiple Şen-innovative trend analyses and partial Mann-Kendall test. *J. Hydrol.* **2018**, *566*, 685–704. [[CrossRef](#)]

34. Yürekli, K. Impact of climate variability on precipitation in the Upper Euphrates–Tigris Rivers Basin of Southeast Turkey. *Atmos. Res.* **2015**, *154*, 25–38. [[CrossRef](#)]
35. Ullah, S.; You, Q.; Ali, A.; Ullah, W.; Jan, M.A.; Zhang, Y.; Xie, W.; Xie, X. Observed changes in maximum and minimum temperatures over China–Pakistan economic corridor during 1980–2016. *Atmos. Res.* **2019**, *216*, 37–51. [[CrossRef](#)]
36. Ramli, F.M.; Aris, Z.A.; Jamil, R.N.; Aderemi, A.A. Evidence of climate variability from rainfall and temperature fluctuations in semi-arid region of the tropics. *Atmos. Res.* **2019**, *224*, 52–64.
37. Theophilou, M.K.; Serghides, D. Estimating the characteristics of the Urban Heat Island Effect in Nicosia, Cyprus, using multiyear urban and rural climatic data and analysis. *Energy Build.* **2015**, *108*, 137–144. [[CrossRef](#)]
38. Livada, I.; Synnefa, A.; Haddad, S.; Paolini, R.; Garshasbi, S.; Ulpiani, G.; Fiorito, F.; Vassilakopoulou, K.; Osmond, P.; Santamouris, M. Time series analysis of ambient air-temperature during the period 1970–2016 over Sydney, Australia. *Sci. Total Environ.* **2019**, *648*, 1627–1638. [[CrossRef](#)]
39. Kumar, P.N.; Rajadurai, A.; Muthuramalingam, T. Multi-Response Optimization on Mechanical Properties of Silica Fly Ash Filled Polyester Composites Using Taguchi–Grey Relational Analysis. *Silicon* **2018**, *10*, 1723–1729. [[CrossRef](#)]
40. Pandya, V.J.; Rathod, P.P. Optimization of mechanical properties of green composites by gray relational analysis. *Mater. Today Proc.* **2020**, *27*, 19–22. [[CrossRef](#)]
41. Yan, Y.; Liu, X.; Wen, Y.; Ou, J. Quantitative analysis of the contributions of climatic and human factors to grassland productivity in northern China. *Ecol. Indic.* **2019**, *103*, 542–553. [[CrossRef](#)]
42. Williams, B.; Brown, T.; Onsmann, A. Exploratory factor analysis: A five-step guide for novices. *Australas. J. Paramed.* **2010**, *8*, 1–13. [[CrossRef](#)]
43. IPCC. *Sixth Assessment Report Climate Change 2021: The Physical Science Basis*; IPCC: Geneva, Switzerland, 2021.
44. Tang, G.; Ding, Y.; Wang, S.; Ren, G.; Liu, H.; Zhang, L. Comparative Analysis of China Surface Air Temperature Series for the Past 100 Years. *Adv. Clim. Chang. Res.* **2010**, *1*, 11–19. [[CrossRef](#)]
45. Ren, G.Y.; Chu, Z.Y.; Chen, Z.H.; Ren, Y.Y. Implications of temporal change in urban heat island intensity observed at Beijing and Wuhan stations. *Geophys. Res. Lett.* **2007**, *34*, L05711. [[CrossRef](#)]
46. Wang, R.; Min, J.; Li, Y.; Hu, Y.; Yang, S. Analysis on Seasonal Variation and Influencing Mechanism of Land Surface Thermal Environment: A Case Study of Chongqing. *Remote Sens.* **2022**, *14*, 2022. [[CrossRef](#)]
47. Founda, D.; Pierros, F.; Petrakis, M.; Zerefos, C. Interdecadal variations and trends of the Urban Heat Island in Athens (Greece) and its response to heat waves. *Atmos. Res.* **2015**, *161–162*, 1–13. [[CrossRef](#)]
48. Zeng, Y.; Qiu, X.F.; Gu, L.H.; He, Y.J.; Wang, K.F. The urban heat island in Nanjing. *Quat. Int.* **2009**, *208*, 38–43. [[CrossRef](#)]
49. Zhang, Y.; Bao, J.W.; Yu, Q.; Ma, C.W. Study on seasonal variations of the urban heat island and its interannual changes in a typical Chinese megacity. *Chin. J. Geophys.* **2012**, *55*, 1121–1128.
50. Liu, W.; Ji, C.; Zhong, J.; Jiang, X.; Zheng, Z. Temporal characteristics of the Beijing urban heat island. *Arch. Meteorol. Geophys. Bioclimatol. Ser. B* **2006**, *87*, 213–221. [[CrossRef](#)]
51. Ramírez-Aguilar, E.A.; Souza, L.C.L. Urban form and population density: Influences on Urban Heat Island intensities in Bogotá, Colombia. *Urban Clim.* **2019**, *29*, 100497. [[CrossRef](#)]
52. Zhang, X.; Li, D.G.; Wu, X.D. Relationship between Urbanization and Urban Heat Island Effect in Zhengzhou. *Urban Environ. Urban Ecol.* **2016**, *5*, 1–6.
53. Chunyan, R.; Dianting, W.; Suocheng, D. The influence of urbanization on the urban climate environment in Northwest China. *Geogr. Res.* **2006**, *25*, 233–241.
54. Yao, R.; Luo, Q.; Luo, Z.; Jiang, L.; Yang, Y. An integrated study of urban microclimates in Chongqing, China: Historical weather data, transverse measurement and numerical simulation. *Sustain. Cities Soc.* **2015**, *14*, 187–199. [[CrossRef](#)]
55. Bao, H.X.H.; Li, L.; Lizieri, C. City profile: Chongqing (1997–2017). *Cities* **2019**, *94*, 161–171. [[CrossRef](#)]
56. Liu, Y.H.; Xu, Y.M.; Zhang, F.M.; Shu, W.J. Influence of Beijing spatial morphology on the distribution of urban heat island. *Acta Geogr. Sin.* **2021**, *76*, 1662–1679.
57. Xiujian, L.; Xuhong, W.; Linzhi, N.; Haiqing, H.; Yurong, Z.; Xiu, Z. Research on the Temporal and Spatial Distribution Characteristics of Urban Heat Island Effect and the Influence of AOD on Urban Heat Island Intensity in the Greater Xi’an Metropolitan Area. *Ecol. Environ. Sci.* **2020**, *29*, 1566–1580.
58. Xu, W.; Yang, H.; Zhang, S. Variations of the urban heat island effect in Shanghai. *J. Trop. Meteorol.* **2018**, *34*, 228–238.
59. Hong, J.W.; Hong, J.; Kwon, E.E.; Yoon, D. Temporal dynamics of urban heat island correlated with the socio-economic development over the past half-century in Seoul, Korea. *Environ. Pollut.* **2019**, *254*, 112934. [[CrossRef](#)] [[PubMed](#)]
60. Fujibe, F. Urban warming in Japanese cities and its relation to climate change monitoring. *Int. J. Climatol.* **2011**, *31*, 162–173. [[CrossRef](#)]
61. Martínez, A.; Reseña de Oke, T.R.; Mills, G.; Christen, A.; Voogt, J.A. *Urban Climates*; Cambridge University Press: Cambridge, UK, 2019; p. 509.
62. Ngarambe, J.; Oh, J.W.; Su, M.A.; Santamouris, M.; Yun, G.Y. Influences of wind speed, sky conditions, land use and land cover characteristics on the magnitude of the urban heat island in Seoul: An exploratory analysis. *Sustain. Cities Soc.* **2021**, *71*, 102953. [[CrossRef](#)]
63. Shi, Y.; Zhang, Y. Urban morphological indicators of urban heat and moisture islands under various sky conditions in a humid subtropical region. *Build. Environ.* **2022**, *214*, 108906. [[CrossRef](#)]

64. He, Z.; Gao, Y.; Yang, S.; Shangguan, C. The Characteristics and Mitigating Measures of Urban Heat Island Effect of Chongqing. *Plat. Mount. Met. Res.* **2017**, *37*, 48–52.
65. Huaijian, X. On Greening Functions: Ecological and Cultural Greening of Urban Roads in Chongqing. *J. Chongqing Jiaotong Univ.* **2007**, *7*, 19–22.
66. Changming, C. Analysis of Planning Measures of Mountain City to Reduce Urban Heat Island. *J. Green Sci. Technol.* **2014**, 282–284.
67. Xinrui, Z.; Qingjuan, N.; Jiangxiu, L. Research on urban geothermal comfort improvement strategy based on ENVI-met. *Ecol. Sci.* **2021**, *40*, 144–155.
68. Cheng, L.; Guan, D.; Zhou, L.; Zhao, Z.; Zhou, J. Urban cooling island effect of main river on a landscape scale in Chongqing, China. *Sustain. Cities Soc.* **2019**, *47*, 101501. [[CrossRef](#)]
69. Jin, C.; Bai, X.; Luo, T.; Zou, M. Effects of green roofs' variations on the regional thermal environment using measurements and simulations in Chongqing, China. *Urban For. Urban Green.* **2018**, *29*, 223–237. [[CrossRef](#)]